

# *Conspicuous endolithic algal associations in a mesophotic reef-building coral*

**Fanny L Gonzalez-Zapata, Sebastián Gómez-Osorio & Juan Armando Sánchez**

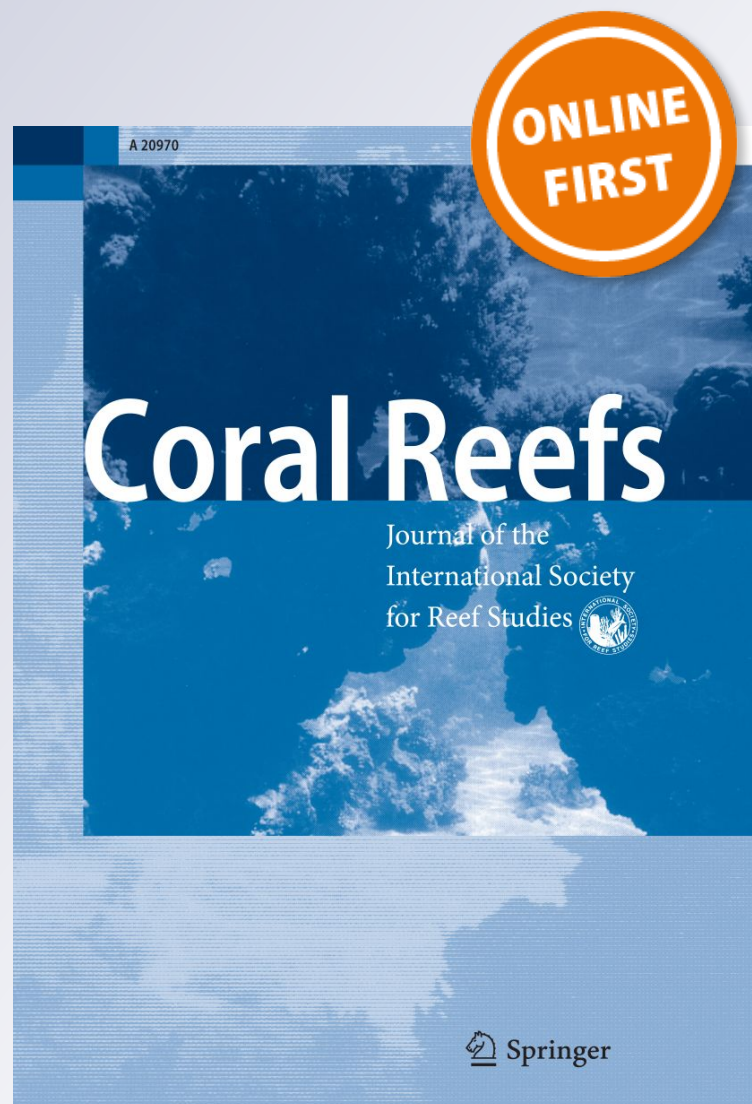
## **Coral Reefs**

Journal of the International Society for Reef Studies

ISSN 0722-4028

Coral Reefs

DOI 10.1007/s00338-018-1695-9



**Your article is protected by copyright and all rights are held exclusively by Springer-Verlag GmbH Germany, part of Springer Nature. This e-offprint is for personal use only and shall not be self-archived in electronic repositories. If you wish to self-archive your article, please use the accepted manuscript version for posting on your own website. You may further deposit the accepted manuscript version in any repository, provided it is only made publicly available 12 months after official publication or later and provided acknowledgement is given to the original source of publication and a link is inserted to the published article on Springer's website. The link must be accompanied by the following text: "The final publication is available at [link.springer.com](http://link.springer.com)".**

## NOTE

# Conspicuous endolithic algal associations in a mesophotic reef-building coral

Fanny L. Gonzalez-Zapata<sup>1</sup>  · Sebastián Gómez-Osorio<sup>1</sup>  · Juan Armando Sánchez<sup>1</sup> 

Received: 20 August 2017 / Accepted: 11 May 2018  
© Springer-Verlag GmbH Germany, part of Springer Nature 2018

**Abstract** Understanding how corals and their symbionts specialize across depth gradients allows us to understand biodiversity in shallow and mesophotic coral ecosystems. Here we determined the prevalence of endolithic algal in *Agaricia undata* (17–83 m) and examined community changes within (shallow, upper and lower zones) and among sites (oceanic vs. continental siliciclastic influence). We observed exposed filaments of endolithic algae in some colonies, which in some cases surfaced the coral as tubular pipelines bridging *A. undata* costae. We also found multiple cryptic species within the monophyletic group of *Ostreobium*-like algae (12 *rbcL* types). Rarely explored as symbionts, *Ostreobium* in *A. undata* highlights its potential role in facilitating a broader depth range.

**Keywords** Mesophotic coral ecosystems · Endolithic algae · Symbiont · *Ostreobium* spp.

## Introduction

The fate of coral reefs has turned into a worldwide concern in the last decades. Yet our current understanding of coral reefs is mainly based on the shallowest quarter of its

overall depth range. This overlooks mesophotic coral ecosystems (MCEs), which occur beyond the limits of regular diving in the so-called twilight zone (> 30 m) (Pyle 1998). Ecological conditions vary over the shallow-mesophotic depth range, which define the distribution of coral communities (Slattery and Lesser 2012). Coral symbiotic associations drive how corals acclimatize to a broader depth range under a climate change scenario. Here, we studied a symbiotic component (endolithic algae) in a coral extending well beyond the lower mesophotic zone.

Symbioses support the framework and resilience of coral reefs. The roles of *Symbiodinium* and bacteria in reef-building species suggest an interdependent holobiont, and still other associations with plantlike forms remain neglected. Endolithic algae, for example, play a dynamic role within the skeleton of scleractinian corals, potentially involved in metabolite translocation (Schlichter et al. 1995), survival during bleaching events (Fine and Loya 2002) and light capture in low-light environments (Koehne et al. 1999; Fine and Loya 2002; Verbruggen and Tribollet 2011). *Ostreobium*-like algae involve physiological traits, which allow corals to thrive at different depths (Gutner-Hoch and Fine 2011). However, the diversity of these endolithic algae in mesophotic coral ecosystems stays largely unnoticed. Here, we provide the first study in the Caribbean of the endolithic algal community in a reef-building coral, *Agaricia undata* (Ellis and Solander 1786), down to the lower mesophotic zone (90 m) extending beyond the compensatory point between photosynthesis and respiration (around 77 m in tropical waters), where zooxanthellate corals face a net loss in productivity (Lesser et al. 2009).

---

Topic Editor Line k Bay

**Electronic supplementary material** The online version of this article (<https://doi.org/10.1007/s00338-018-1695-9>) contains supplementary material, which is available to authorized users.

---

✉ Juan Armando Sánchez  
juansanc@uniandes.edu.co

<sup>1</sup> Departamento de Ciencias Biológicas (Biommar), Facultad de Ciencias, Universidad de los Andes, Bogotá, Colombia

## Materials and methods

### Sample collection

To estimate the prevalence and diversity of endolithic algal associations in *A. undata*, 103 colony fragments were collected between 2015 and 2016 in three Colombian locations: San Andres island (N12°32'34.112" W081°42'41.079") in April and June 2015 and March 2016, Cartagena (N10°15'55.944" W075°37'32.915") in July and November 2015 and Natural National Park 'Corales de Profundidad' (N10°06'29.3" W076°0'33.998") in December 2015, the first location with oceanic influence and the last two, about 500 km apart, with continental siliciclastic influence due to river runoff. The oceanic and siliciclastic conditions have notable differences in light penetration but similar temperature regimes without strong seasonal changes (Velásquez and Sánchez 2015). Depths of sample collection ranged between 17 and 83 m and were obtained using SCUBA or Closed Circuit Rebreather with Trimix below 40 m. Dives in the mesophotic zone (planned to 100 m, one per day) allowed us only 20–30 min of bottom time (Trimix 10/60, oxygen/helium) and about 2.5 h of decompression time. The samples were grouped in three categories: shallow ( $\leq 30$  m), upper ( $> 30$  and  $< 60$  m) and lower ( $\geq 60$  m) zones (see details in Electronic Supplementary Material, ESM Table S1). Although sampling numbers seem low, in comparison with shallow-water projects, here we included the entire depth range of the species at each locality and we restricted sampling to colonies at least 5 m apart, which reduced encountering clones. A coral subsample ( $\sim 2 \times 2$  cm) was collected for each colony; a small fragment ( $0.5 \times 0.5$  cm<sup>2</sup>) was preserved in individual tubes with DMSO salt buffer (0.5 M EDTA; 20% (v/v) DMSO, saturated with NaCl) and stored at  $-80$  °C until DNA extraction. A dry voucher is available at the Museo de Historia Natural ANDES (ANDES-IM 4681–4784). Research and collection of specimens were approved by the National Environmental Licensing Authority (ANLA, Spanish acronym): Collection Framework Agreement granted to Universidad de los Andes through resolution 1177 of October 9, 2014-IBD 0359.

### Scanning electron microscopy (SEM) and energy-dispersive X-ray spectroscopy (EDS)

Using light microscopy, we determined the presence by visual estimation of the endolithic algal in the coral dry fragment, filaments connecting the costae (henceforth refer as a 'pipeline'), and calcified dead filaments were identified. A motor tool was used to cut fragments of around 1 cm<sup>2</sup>. Each fragment was fixed in 2.5% glutaraldehyde and 0.5%

formaldehyde made in 0.1 M phosphate buffer at pH 7.2 for 36 h (Golubic et al. 2005). After fixation, samples were washed with distilled water and dehydrated with an ethanol series of 50, 70, 90 and 96%, 1 h each ethanol concentration. A total of six samples with high concentration of 'pipelines' and dead filaments were fixed for the EDS analysis. The samples were dried with critical dry point and coated with gold before SEM, and then, EDS was executed. Coral bridge basements (coral skeleton) were used as controls, to compare coral, dead filaments and 'pipeline' composition.

### DNA extraction, amplification and analysis

DNA was extracted using the CTAB protocol (Coffroth et al. 1992). For PCR amplification, we used the following primers: *rbcLF* ('5-ATHGARCCNGTNGTNGGNGAR-3') and *rbcLR* ('5-CNGTYTCNGCYTGNGCYTTRTA-3'). The chloroplast gene ribulose 1,5-bisphosphate carboxylase large subunit (*rbcL*) has been used successfully to determine the genotypic diversity of *Ostreobium* within scleractinian corals (Gutner-Hoch and Fine 2011). PCR was performed in a 15  $\mu$ l reaction containing 1 $\times$  PCR buffer, 3 mM MgCl<sub>2</sub>, 1  $\mu$ l of 10 $\times$  bovine serum albumin (BSA 20 mg/ $\mu$ l), 0.16 mM of each dNTP, 0.52 mM of each primer, 1 U Taq DNA polymerase and 1  $\mu$ l of DNA (30 ng). PCR conditions were 94 °C for 2 min followed by 35 cycles of 94 °C for 90 s, 52 °C for 90 s and 72 °C for 60 s and a 5-min extension at 72 °C. Resulting PCR products were cleaned with FastAP Thermosensitive Alkaline Phosphatase (Thermo Scientific™) and sequenced using the BigDye Terminator v3.1 Cycle Sequencing Kit (Applied Biosystems) on the AB13730xl DNA Analyzer (Applied Biosystems). GenBank Accession No. MF135622-MF135643.

Sequence alignment analysis was performed using the AliView software (Larsson 2014). Evolutionary model was assessed using Jmodeltest 2.1.2 (Guindon and Gascuel 2003; Durriba et al. 2012) which resulted in HKY + I + gamma according to the BIC calculations. We reconstructed phylogenetic relationships with two methods: Bayesian inference with BEAST v1.8.2 (Drummond et al. 2012) and MrBayes v3.2.2 (Ronquist et al. 2012) and maximum likelihood trees were estimated using RaxML (Stamatakis 2006). Both methods resulted in the same tree topology; thus, only the Bayesian tree is reported here. Three methods were used to identify phylopecies or clades: generalized mixed Yule coalescent model in our Bayesian ultrametric trees using the R package bGMYC (Reid and Carstens 2012), coalescent Poisson tree process (PTP) method (Zhang et al. 2013) and pairwise genetic distance using MEGA6 (Tamura et al. 2013). bGMYC analysis was based on 100 trees from the post-burn-in generations obtained from the BEAST analysis. For each of

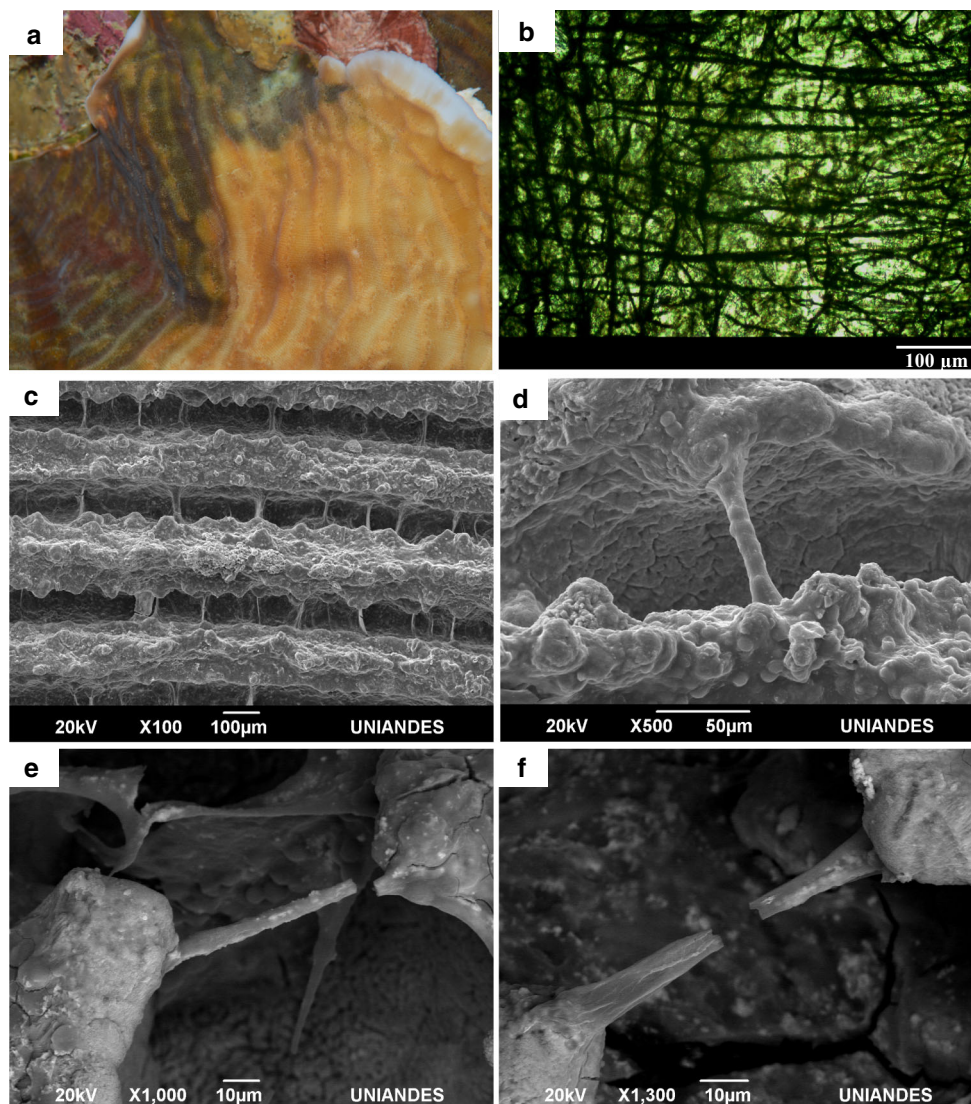
the 100 trees, the Markov chain Monte Carlo sampler was run for 50,000 generations, discarding the first 40,000 generations as burn-in and sampling every 100 generations. The upper threshold, defined as number of tips on the tree, was set to 48, and a cutoff value was set as 0.5 to delimit the lineages. For PTP method (Zhang et al. 2013), we used the web interface <http://species.h-its.org> with Bayesian tree as input, 100,000 MCMC generations, thinning every 100 generations and a burning fraction of 0.1. Endolithic algal clades were named following and continuing the nomenclature used by (Gutner-Hoch and Fine 2011) in which each clade is represented by a letter of the alphabet followed by numbers for the internal grouping. *rbcL* sequences of clade A-G (JF801728–JF801734) reported by Gutner-Hoch and Fine (2011) in the Red Sea were included for the reconstruction of the phylogenetic relationships. *Caulerpa webbiana* (AB054017) were included as an outgroup for the Bryopsidales order.

## Results and discussion

Endolithic algae were macroscopically observed in 58% ( $n = 103$ ) of *A. undata* sampled (Fig. 1a), but of those, only 28 samples amplified the *rbcL* gene (despite multiple attempts). Microscopic assessment of the endolithic interface demonstrated a close association clearly reaching the coral surface. Thin sections revealed that these algae have a network pattern that grows parallel to the coral surface (Fig. 1b). Some exposed algal filaments emerged as a tubular pipeline bridging the network through coral costae (Fig. 1c–f). Although we did not register colony size, largest colonies had endolithic algae reaching the coral surface in centrally located tissues.

Energy-dispersive X-ray spectroscopy (EDS) identified the elemental composition of the filaments, which composition differed between the ‘pipeline’ and the coral tissue (Supplementary Fig. S1). Coral skeleton involved carbon

**Fig. 1** Morphological observations of the filaments of the algae by light microscopy and scanning electron microscope (SEM). **a** Detail of the endolithic algae showing dense coverage in the base of colony, **b** view of a longitudinal section of coral cut, **c** coral—*Ostreobium* tubular pipeline between costae, **d**, **e** higher magnification of the filament pipeline bridging two costae, **f** clearly shrunk filament pipeline, after the EDS electron beam



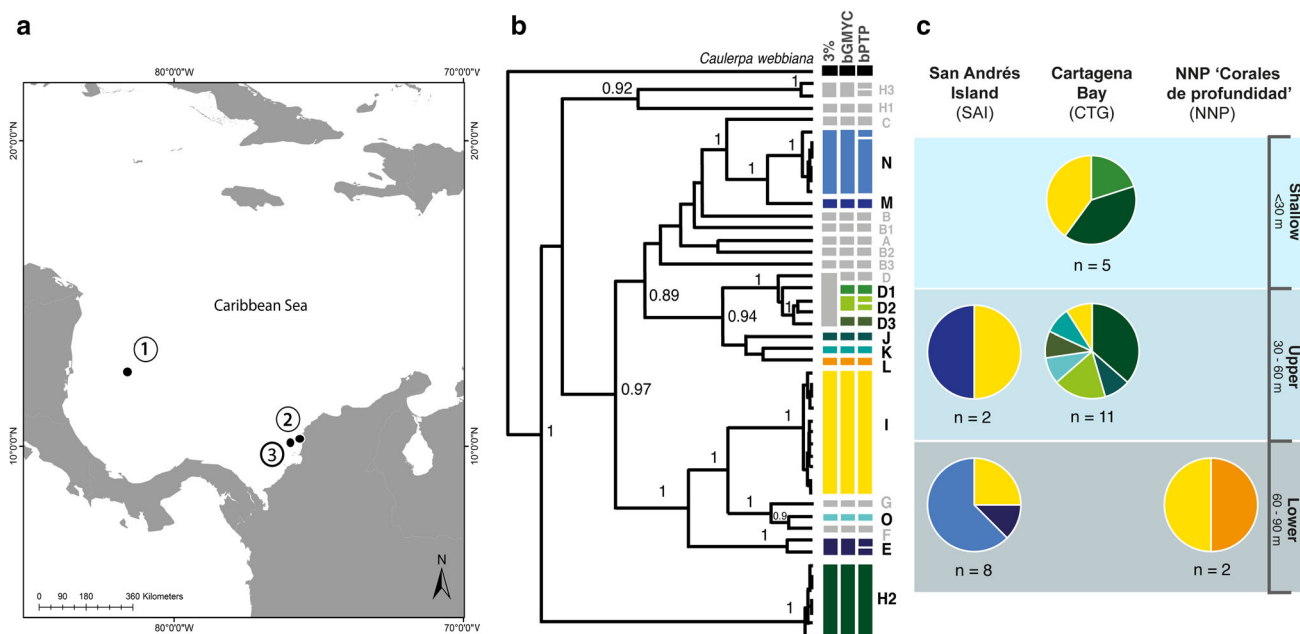


**Fig. 2** Sampling locations, genetic diversity and relative abundance of endolithic boring algae in *Agaricia undata* across depths and locations. **a** Map showing sampled populations in the Caribbean Sea off the coast of Colombia. (1) San Andrés, (2) Cartagena and (3) Natural National Park ‘Corales de Profundidad.’ **b** Bayesian MCMC phylogenetic tree of *Ostreobium*-like algae OTUs based on chloroplast gene *rbcL* and clades previously reported by Gutner-Hoch E, Fine M (2011). Colored bars to the right of the phylogeny represent

OTUs grouping based on genetic distance thresholds (3%), bGMVC and bPTP with their corresponding clade nomenclature, where gray bars represent clades of endolithic algae found in other species different to *A. undata*. Bootstrap values are based on Bayesian analyses, with only probabilities over 80% shown. **c** Pie charts summarizing diversity and distribution of algae OTUs across depth range per locality, which colors correspond to the clades defined in a

(C), calcium (Ca) and oxygen (O), but the filament pipeline, bridging costae, had additional compounds like sulfur (S) and potassium (K). Sulfur could be associated with small cysteine-rich proteins (SCRiPs) in the membrane of calcifying organisms (Sunagawa et al. 2009). *Ostreobium* spp. could be using the  $\text{CaCO}_3$  waste of the boring process to make these pipeline-like structures, across *A. undata* costae, to improve the light uptake in the mesophotic zone. All tubular structures nearly shrunk after the electron beam of the EDS sampled (Fig. 1f).

Phylogenetic analyses of the chloroplast *rbcL* region (395 bp) from endolithic algae revealed a community consisting of 12 phylospecies/clades (Fig. 2a). Multiple endolithic algae types were found in association with *A. undata*. Some clades were geographically structured, whereas others distributed worldwide, (H2 and E) previously reported by Gutner-Hoch and Fine (2011), or showed little ecological structure (type I). In Cartagena, we found eight *Ostreobium*-like algae; five of these (D2, D3, J, K and O) were exclusive to the upper zone and one to shallow water (D1). In San Andrés, two (E and N) out of four OTUs were limited to the lower zone and one to the upper zone (M) (Fig. 2b). *Ostreobium* DNA was also found in the pipeline-like structure, which corresponded to clades N and H2.

The notion that the green band found in the skeleton of corals belongs to one cosmopolitan species (*Ostreobium quekettii*) is inaccurate. As in Gutner-Hoch and Fine (2011) and Sauvage et al. (2016), we found multiple cryptic species within the monophyletic group of *Ostreobium*-like algae. *Ostreobidinea* diversity in *A. undata* (12 clades) was higher than previously observed, while previous work found seven clades in two species (Gutner-Hoch and Fine 2011). Except for clade I that was found in all localities and along a wide range (17–80 m), *Ostreobium* spp. was partitioned by the reef setting, i.e., oceanic or continental siliciclastic influence, which is expected in response to low-light, organic matter and/or macroscopic predators (Sauvage et al. 2016), which are different at the two types of Caribbean reefs (Velásquez and Sánchez 2015). In a parallel study using the same samples, we found that both *Symbiodinium* and *Ostreobium* had similar and consistent regional variations in *A. undata* populations, suggesting an analog host–symbiont specificity. Remarkably, there were more types of *Ostreobium* associated with *A. undata* than to *Symbiodinium* (types: 12 vs. 7; *n*: 28 vs. 77) despite the fact that more samples were screened for zooxanthellae (Gonzalez-Zapata et al. 2018).

*Ostreobium*-like algae impose a paradox for coral reef science, where the most pervasive microbioeroder of coral

skeletons (Tribollet 2008) as it reaches the coral tissue apparently coexists with the coral colony. These algae infest corals at different depths but are particularly shade-adapted (Ralph et al. 2007). The previous research has shown that *Ostreobium* spp. under extreme low light, as in MCEs, can absorb red and far-red wavelengths and change the chl *b*:chl *a* ratio according to depth (Shashar and Stambler 1992; Magnusson et al. 2007). These algae use coral metabolic waste and can translocate fixed carbon to the coral host during stress events or at extreme depths, which indicates commensalistic to mutualistic interactions (Fine and Loya 2002). This should be tested experimentally, but the high diversity and differences found over depth could be a key factor for *A. undata* to colonize mesophotic ecosystems. Since not all colonies presented this association, further testing is needed to determine whether there is a successional process occurring, as *Ostreobium* was most often noted in older colonies of *A. undata*.

**Acknowledgements** This study was supported by COLCIENCIAS Grant No. 120465944147, Universidad de los Andes (Vicerrectoria de Investigaciones-Programa de Investigación en Especiación Ecológica) and CORALINA (Convenios 13-2014 and 21-2015). We thank N. Bolaños, E. Castro, J. Andrade, F. García, O. Ruiz, D. Seguro, L. Dueñas, M. Forero, L. Gutierrez, M. Gómez, M. Marrugo, P. Bongaerts, C. Ramirez and A. Henao.

#### Compliance with ethical standards

**Conflict of interest** The authors declare they have no conflicts of interest.

## References

- Coffroth MA, Lasker HR, Diamond ME, Bruenn JA, Birmingham E (1992) DNA fingerprints of a gorgonian coral: a method for detecting clonal structure in a vegetative species. *Mar Biol* 114:317–325
- Darriba D, Taboada GL, Doallo RR, Posada D (2012) jModelTest 2: more models, new heuristics and parallel computing. *Nat Methods* 9:772
- Drummond AJ, Suchard MA, Xie D, Rambaut A (2012) Bayesian phylogenetics with BEAUti and the BEAST 1.7. *Mol Biol Evol* 29:1969–1973
- Ellis J, Solander DC (1786) The natural history of many curious and uncommon zoophytes: collected from various parts of the globe. B. White and Peter Elmsly
- Fine M, Loya Y (2002) Endolithic algae: an alternative source of photoassimilates during coral bleaching. *Proc Biol Sci* 269:1205–1210
- Golubic S, Radtke G, Le Campion-alsumard T, Le Campion-alsumard T (2005) Endolithic fungi in marine ecosystems. *Trends Microbiol* 13:229–235
- Gonzalez-Zapata FL, Bongaerts P, Ramírez-Portilla C, Adu-Oppong B, Walljasper G, Reyes A, Sanchez JA (2018) Holobiont diversity in a reef-building coral over its entire depth range in the mesophotic zone. *Front Mar Sci* 5:29
- Guindon S, Gascuel O (2003) A simple, fast, and accurate algorithm to estimate large phylogenies by maximum likelihood. *Syst Biol* 52:696–704
- Gutner-Hoch E, Fine M (2011) Genotypic diversity and distribution of *Ostreobium quekettii* within scleractinian corals. *Coral Reefs* 30:643–650
- Koehne B, Elli G, Jennings RC, Wilhelm C, Trissl HW (1999) Spectroscopic and molecular characterization of a long wavelength absorbing antenna of *Ostreobium* sp. *Biochim Biophys Acta Bioenergy* 1412:94–107
- Larsson A (2014) AliView: a fast and lightweight alignment viewer and editor for large datasets. *Bioinformatics* 30:3276–3278
- Lesser MP, Slattery M, Leichter JJ (2009) Ecology of mesophotic coral reefs. *J Exp Mar Bio Ecol* 375:1–8
- Magnusson S, Fine M, Kühl M (2007) Light microclimate of endolithic phototrophs in the scleractinian corals *Montipora monasteriata* and *Porites cylindrica*. *Mar Ecol Prog Ser* 332:119–128
- Pyle RL (1998) Use of advanced mixed-gas diving technology to explore the coral reef “twilight zone”. In: *Ocean pulse*, pp 71–88
- Ralph PJ, Larkum AWD, Kühl M (2007) Photobiology of endolithic microorganisms in living coral skeletons: 1. Pigmentation, spectral reflectance and variable chlorophyll fluorescence analysis of endoliths in the massive corals *Cyphastrea serailia*, *Porites lutea* and *Goniastrea australensis*. *Mar Biol* 152:395–404
- Reid NM, Carstens BC (2012) Phylogenetic estimation error can decrease the accuracy of species delimitation: a Bayesian implementation of the general mixed Yule-coalescent model. *BMC Evol Biol* 12:196
- Ronquist F, Teslenko M, Van Der Mark P, Ayres DL, Darling A, Höhna S, Larget B, Liu L, Suchard MA, Huelsenbeck JP (2012) MrBayes 3.2: efficient bayesian phylogenetic inference and model choice across a large model space. *Syst Biol* 61:539–542
- Sauvage T, Schmidt WE, Suda S, Fredericq S (2016) A metabarcoding framework for facilitated survey of endolithic phototrophs with tufA. *BMC Ecol* 16:8
- Schlichter D, Zscharnack B, Krisch H (1995) Transfer of photoassimilates from endolithic algae to coral tissue. *Naturwissenschaften* 82:561–564
- Shashar N, Stambler N (1992) Endolithic algae within corals-life in an extreme environment. *J Exp Mar Biol Ecol* 163:277–286
- Slattery M, Lesser MP (2012) Mesophotic coral reefs: a global model of community structure and function. In: *Proceedings of 12th international coral reef symposium Cairns*, pp 9–13
- Stamatakis A (2006) RAxML-VI-HPC: maximum likelihood-based phylogenetic analyses with thousands of taxa and mixed models. *Bioinformatics* 22:2688–2690
- Sunagawa S, Desalvo MK, Voolstra CR, Reyes-bermudez A (2009) Identification and gene expression analysis of a taxonomically restricted cysteine-rich protein family in reef-building corals. *PLoS One* 4:e4865
- Tamura K, Stecher G, Peterson D, Filipowski A, Kumar S (2013) MEGA6: molecular evolutionary genetics analysis version 6.0. *Mol Biol Evol* 30:2725–2729
- Tribollet A (2008) The boring microflora in modern coral reef ecosystems: a review of its roles. Current developments in bioerosion. Springer, Berlin, Heidelberg, pp 67–94
- Velásquez J, Sánchez JA (2015) Octocoral species assembly and coexistence in Caribbean coral reefs. *PLoS ONE* 10:e0129609
- Verbruggen H, Tribollet A (2011) Boring algae. *Curr Biol* 21:R876–R877
- Zhang J, Kapli P, Pavlidis P, Stamatakis A (2013) A general species delimitation method with applications to phylogenetic placements. *Bioinformatics* 29:2869–2876